TÜBİTAK

Turk J Elec Eng & Comp Sci, Vol.20, No.3, 2012, © TÜBİTAK
doi:10.3906/elk-1008-684

Performance analysis of wind turbine-driven permanent magnet generator with matrix converter

Ramasamy BHARANIKUMAR[1,*], **A. Nirmal KUMAR**[2]
[1] *Department of Electrical and Electronics Engineering, Bannari Amman Institute of Technology, Anna University, Tamil Nadu-INDIA*
e-mails: bharani_rbk@rediffmail.com, bharanikumar.rbk@gmail.com
[2] *Department of Electrical and Electronics Engineering, INFO Institute of Engineering, Anna University, Tamil Nadu-INDIA*
e-mail: ankhod@gmail.com

Received: 17.08.2010

Abstract

Wind energy, among all of the renewable energy sources, has made rapid developments and significant inroads in electrical power systems. With the increased use of wind energy conversion systems (WECSs), several technologies have been developed. Since WECSs are more cost competitive, the comparison of different wind generator systems is the need of the hour. Permanent magnet generators employing these technologies have some significant advantages over conventional generators, such as no need of excitation, low volume and weight, high precision, and deletion of the gearbox. A variable-speed WECS with a permanent magnet generator and a matrix converter is proposed in this paper. The traditional power conversion stages consist of a rectifier followed by an inverter and bulky DC link capacitor. It involves 2 stages of power conversion and, subsequently, the efficiency of the overall WECS is reduced because of power quality issues mainly based on total harmonic distortion. The matrix converter is mainly utilized to control the output voltage and frequency, and its input current and output voltage are closer to a sine wave. The matrix converter is a simple and compact AC-AC converter. The proposed WECS with matrix converter is modeled using PSIM and results were checked with an experimental setup.

Key Words: *Wind turbine, permanent magnet generator, matrix converter, rectifier, inverter*

1. Introduction

A growing proportion of energy is being met all over the world by electricity. This trend will be increasing day by day as the demand for electricity is increasing. This demand will have an increased impact on developing countries because their industrial progress will be based on modern technological developments in power generation. During recent years, due to the depletion of fossil fuels and the environmental problems

*Corresponding author: Department of Electrical and Electronics Engineering, Bannari Amman Institute of Technology, Anna University, Tamil Nadu-INDIA

caused by the use of fossil fuels, renewable energy sources have become the most sought resources. Wind is one of the sources of renewable energy [1-3]. Wind power is converted to electricity by wind turbine generators. Various technologies have been developed in wind energy conversion systems (WECSs) as the result of the effort to further improve WECSs based on the permanent magnet generator (PMG). Induction generators are most widely used in WECSs. Although they are robust and inexpensive, the space-consuming capacitors are bulky and expensive [4,5]. Induction generators with step-up gearboxes have low efficiency at low speeds [6]. When compared to conventional generators, the PMGs have the advantages of being robust in construction, very compact in size, not requiring an additional power supply for magnetic field excitation, and requiring less maintenance. A variable-speed WECS including a PMG offers advantages over the constant-speed approach, such as maximum power-point tracking capability and reduced acoustic noise at lower wind speeds [7,8]. Figure 1 shows the block diagram of a variable-speed traditional WECS. It consists of a wind turbine and PMG, followed by the rectifier and inverter. The DC link consists of a bulky capacitor.

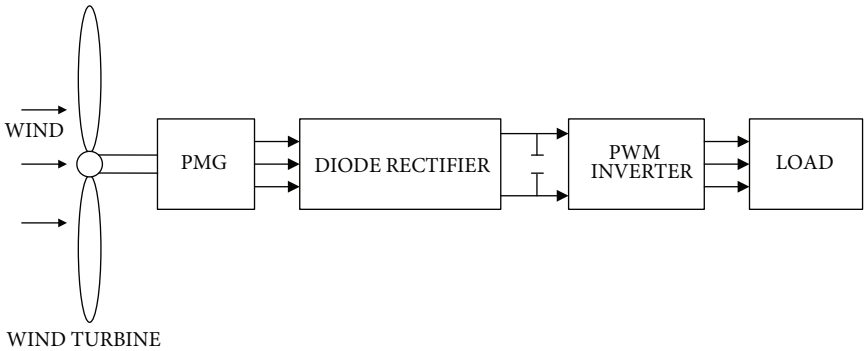

Figure 1. Conventional WECS.

Figure 2 shows the block diagram of the proposed wind turbine-driven, PMG-fed matrix converter. When compared with conventional AC-DC-AC converters, the proposed WECS with the matrix converter has the following advantages:

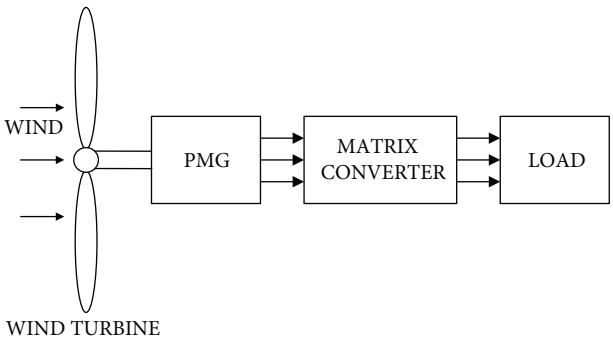

Figure 2. Block diagram of proposed WECS.

- The matrix converter provides almost sinusoidal waveforms in the input and output sides. The absence of a DC link capacitor means that the matrix converter has a compact design and less weight [6,9].
- At low switching frequencies, the efficiency of matrix converter-based WECSs is higher than that of conventional WECSs, and the matrix converter has faster dynamic response [10].

- The matrix converter is highly controllable and allows for independent control of the output voltage magnitude and frequency and the input power factor [10,11].
- The intermediate DC link creates an electrical decoupling between the PMG and the grid. Hence, it requires a separate controller for compensation of stored kinetic energy in the wind turbine [12].

This paper focuses on the modeling of a wind turbine-driven PMG with a matrix converter, developed in PSIM. The simulation is analyzed based on turbine speed, generator output voltage, and frequency for different values of input wind velocities. Dynamic analysis is also conducted for sudden variations of wind speed. The performance of the matrix converter is controlled using a sinusoidal pulse width modulation (SPWM)-based controller. Finally, the simulated results are verified with experimental results. This paper also presents comparisons of the proposed WECS with a conventional 2-stage WECS based on input, output total harmonic distortion (THD), and efficiency.

2. Components of proposed WECS

2.1. Wind turbine model

Wind turbines are classified into vertical axis types and horizontal axis types. Most modern wind turbines use the horizontal axis configuration due to the advantages of low cost, high efficiency, and ease in design for high power ratings. The output power of the wind turbine is given as in Eq. (1) [8,13]:

$$P = \frac{1}{2}\pi\rho R^2 V_w^3 C_p, \tag{1}$$

where P is the mechanical output power of the wind turbine (W), ρ is the air density in kg/m^3, R is the radius of the turbine (m), V_w is the wind speed (m/s), and C_p is the power coefficient of the turbine, which in turn is a function of tip speed ratio λ and blade pitch angle β (degrees). The tip speed ratio is the ratio of blade tip speed to wind speed. C_p is expressed as a function of the tip speed ratio λ, given by Eq. (2) [4,5].

$$\lambda = \frac{R\omega_t}{V_w} \tag{2}$$

It is important to note that the aerodynamic efficiency is maximal at the optimum tip speed ratio. The torque expression is obtained from equation Eq. (1) by dividing the turbine speed. It is given in Eq. (3):

$$T_t\left(V_w, \omega_t\right) = \frac{1}{2}\pi p R^3 C_t\left(\lambda\right) V_w^2, \tag{3}$$

where $C_t\left(\lambda\right)$ is the torque coefficient of the turbine, given by Eq. (4).

$$C_t\left(\lambda\right) = \frac{C_p\left(\lambda\right)}{\lambda} \tag{4}$$

The power coefficient C_p [8] is given by Eq. (5) [13]:

$$C_p\left(\lambda\right) = \left(\frac{116}{\lambda 1} - \left(0.4 \times \beta\right) - 5\right) 0.5 e^{\frac{-16.5}{\lambda 1}}, \tag{5}$$

where:

$$\lambda_1 = \frac{1}{\left(\frac{1}{(\lambda+0.089\,\beta)} - \frac{0.035}{\beta^3+1}\right)}.$$

The model of the wind turbine is described by the following differential equations:

$$\frac{d\omega_t}{dt} = \frac{1}{j_t}\left[T_t\left(V,\omega_t\right) - T_s\right], \tag{6}$$

$$\frac{dT_s}{dt} = K_s\left[\omega_t - \omega_g\right] + \frac{B_s}{J_t}\left[T_t\left(V,\omega_t\right) - T_s\right] + \frac{B_s}{J_g}\left[T_g\left(cos\alpha\,,\,\omega_g\right) - T_s\right], \tag{7}$$

$$\frac{d\omega_g}{dt} = \frac{1}{j_g}\left[T_g - T_s\right]. \tag{8}$$

The basic components of the wind electric system are the wind turbine, PMG, and matrix converter, shown in Figure 2. The generated power in the PMG is fed to the load through the matrix converter. Since the wind power fluctuates with wind velocity, the generator output voltage frequency varies continuously. The matrix converter converts the desired value of voltage and frequency.

2.2. Modeling of a direct-driven PMG

A specific model of the machine is required to determine the steady state and transient behavior of the PMG. The model of the PMG can be obtained by means of 2-phase machines in direct and quadrature axes. The equivalent circuit for the q-axis and d-axis model of the PMG with the rotor reference frame is shown in Figures 3 and 4, respectively [2,14].

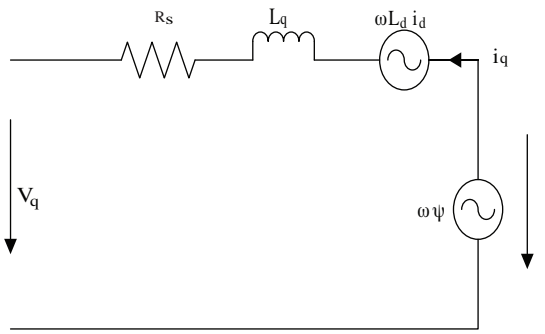

Figure 3. Quadrature axis model of PMG.

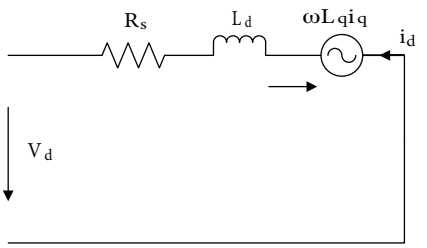

Figure 4. Direct axis model of PMG.

The expression for the terminal voltage of the PMG obtained from the above d-q model may be expressed in matrix form as follows:

$$\left[V_{abc}\right] = -\left[R_{abc}\right]\left[i_{abc}\right] + \rho\left[\psi_{abc}\right] \quad . \tag{9}$$

The complete model of the generator is derived in d-q coordinates. The voltage equations for the d and q axes [14] are given by Eqs. (10) and (11).

$$V_d = -R_s i_d - L_d\frac{d}{dt}i_d + \omega_r L_q i_q \tag{10}$$

$$V_q = -R_s i_q - L_q \frac{d}{dt} i_q - \omega_r L_d i_d + \omega_r \psi_m \tag{11}$$

The position of the magnets in the rotor determines, independently of stator voltages and currents, the instantaneously induced electromagnetic fields and subsequently the stator currents and torque of the machine [1,5]. Hence, the rotor reference frame is preferred.

The electromagnetic torque developed in the PMG is given in Eq. (12).

$$T_e = \left(\frac{3}{2}\right)\left(\frac{P}{2}\right)\left[\left(L_d - L_q\right)\, i_q i_d - \psi_m i_q\right] \tag{12}$$

The input torque with respect to the torque developed in the wind turbine and the rotor angular velocity of the generator, ω_r, is described by Eq. (13).

$$T_i = J\left(\frac{2}{P}\right)\rho\omega_r - T_e \tag{13}$$

Assume that the air gap is uniform and the stator inductances of the q and d axes windings are equal to L_s. The output voltages of the PMG in the rotor reference frame are $V_q = V_S$, $V_d = 0$. Under this assumption, by substituting the above values, the voltage equation in the q-axis and electromagnetic torque may be expressed as follows [4,13]:

$$V_s = -\left(R_s + \rho L_s\right)\, i_q + \omega_r \psi_m, \tag{14}$$

$$T_e = \left(\frac{3}{2}\right)\left(\frac{P}{2}\right)\left[-\psi_m i_q\right]. \tag{15}$$

The equations discussed above were implemented in the PSIM environment. In order to simplify the implementation, the main computational part was written in a function format. The relationship between the rotor angular velocity of the generator, ω_r, and the mechanical angular velocity of the rotor, ω_m, may be expressed as in Eq. (16).

$$\omega_r = \frac{P}{2}\omega_m \tag{16}$$

The rotational speed and torque are given in Eq. (17).

$$T_i = J\frac{d\omega_m}{dt} - T_e \tag{17}$$

From Eqs. (14) and (15),

$$T_i = J\left(\frac{2}{P}\right)\rho\omega_r - T_e. \tag{18}$$

The output voltage from the PMG is sinusoidal, such that:

$$V_a = V_s cos\theta_r, \tag{19}$$

$$V_b = V_s cos\left(\theta_r - 120^0\right), \tag{20}$$

$$V_c = V_s cos\left(\theta_r + 120^0\right). \tag{21}$$

The expression of Eqs. (14), (15), and (16) in a rotor reference frame may be written as in Eqs. (22) and (23).

$$V_q = V_s \tag{22}$$

$$V_d = 0 \tag{23}$$

Under the assumption of a uniform air gap, self-inductance is independent of angular position; hence, it is constant. For a practical PMG, $L_d = L_q = L_s$. Under this assumption, by substituting Eqs. (20) and (21) into Eqs. (8), (9), and (10), the voltage equation in the q-axis and electromagnetic torque can be written as in Eqs. (24) and (25).

$$V_q = -\left[\frac{(R_s+\rho L_s)^2+\omega_r^2 (L_s)^2}{R_s+\rho L_s}\right] i_q+\omega_r \psi_m \tag{24}$$

$$T_e = \left(\frac{3}{2}\right)\left(\frac{P}{2}\right)[-\psi_m i_q] \tag{25}$$

If $\omega_r^2 (L_s)^2$ is neglected, Eq. (24) is linear. It may then be rewritten as:

$$V_q = -(R_s+\rho L_s)\, i_q+\omega_r \psi_m. \tag{26}$$

The model discussed above was implemented in the PSIM environment.

2.3. Matrix converter

A matrix converter is the most versatile converter without any limits on the output voltage and frequency. A matrix converter is a forced commutated converter, which uses an array of bidirectional switches. The matrix converter creates a variable output voltage with unrestricted frequency [10,15,16]. It replaces the conventional 2-stage power converters and the intermediate energy storage element and high-quality power output waveforms [11]. A 3-phase matrix converter requires 9 bidirectional switches capable of blocking voltage and conducting current in both directions. The bidirectional switches usually consist of 2 insulated gate bipolar transistors (IGBTs) connected in an antiparallel fashion [15,17,18]. A basic matrix converter with PMG topology is shown in Figure 5.

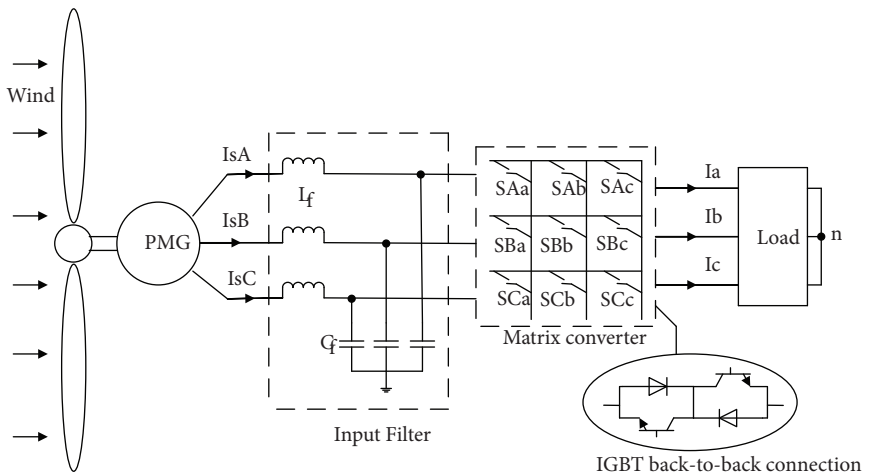

Figure 5. Proposed WECS with matrix converter.

It has an array with an m × n combination, directly connecting the m-phase voltage source to an n-phase load. Figure 5 shows a 3 × 3 matrix converter using 9 switches. In the Venturini method, the appropriate firing pulses to each of the 9 bidirectional switches must be calculated to generate sinusoidal output voltages and variable frequency [14,19]. In this paper, Vjn, j = {a,b,c} are the load voltages with respect to neutral point n of the load; Ij, j ={a,b,c} are the load currents. The matrix converter input voltage is Vi, i = {A,B,C}, and the input current is ii, i = {A,B,C}.[6,16].

The modulation matrix is given in Eq. (27).

$$M(t) = \begin{bmatrix} m_{Aa}(t) & m_{Ba}(t) & m_{Ca}(t) \\ m_{Ab}(t) & m_{Bb}(t) & m_{Cb}(t) \\ m_{Ac}(t) & m_{Bc}(t) & m_{Cc}(t) \end{bmatrix} \tag{27}$$

The sinusoidal input voltages of the matrix converter are given in Eq. (28).

$$\overline{v}_i = \begin{bmatrix} cos(\omega_i t) \\ cos(\omega_i t - 2\pi/3) \\ cos(\omega_i t + 2\pi/3) \end{bmatrix} \tag{28}$$

The sinusoidal output currents of the matrix converter can be given as in Eq. (29).

$$\overline{i_o} = I_{om} \begin{bmatrix} cos(\omega_o t + \phi_o) \\ cos(\omega_o t + \phi_o - 2\pi/3) \\ cos(\omega_o t + \phi_o + 2\pi/3) \end{bmatrix} \tag{29}$$

Here, ϕ_o is the output current phase angle.

In accordance with this, each output phase voltage can be expressed as in Eq. (30).

$$[v_{jN}(t)] = [M(t)]\,[v_i(t)] \tag{30}$$

In the same way, the input current is given as in Eq. (31).

$$[i_i(t)] = [M(t)]^T\,[i_o(t)] \tag{31}$$

Here, $[M(t)]^T$ is the transpose matrix of $[M(t)]$. The duty cycles of the bidirectional switches were calculated according to:

$$t_{Kj} = T_s \left[\frac{1}{3} + \frac{2_{v_k v_j}}{3v_{im}^2} + \frac{2q}{9q_m} sin(\omega_i t + \beta_k) sin(3\omega_i(t)\right], \tag{32}$$

K= {A,B,C}; j= {a,b,c}, $\beta = 0, \frac{2\pi}{3}, \frac{4\pi}{3}$.

3. Simulation results

Figure 6 shows the PSIM-simulated model of a conventional 2-stage power conversion system for a wind turbine-driven PMG. The model was simulated for different values of wind velocity and different loading conditions. Finally, the input and output THD was compared with that of the proposed WECS.

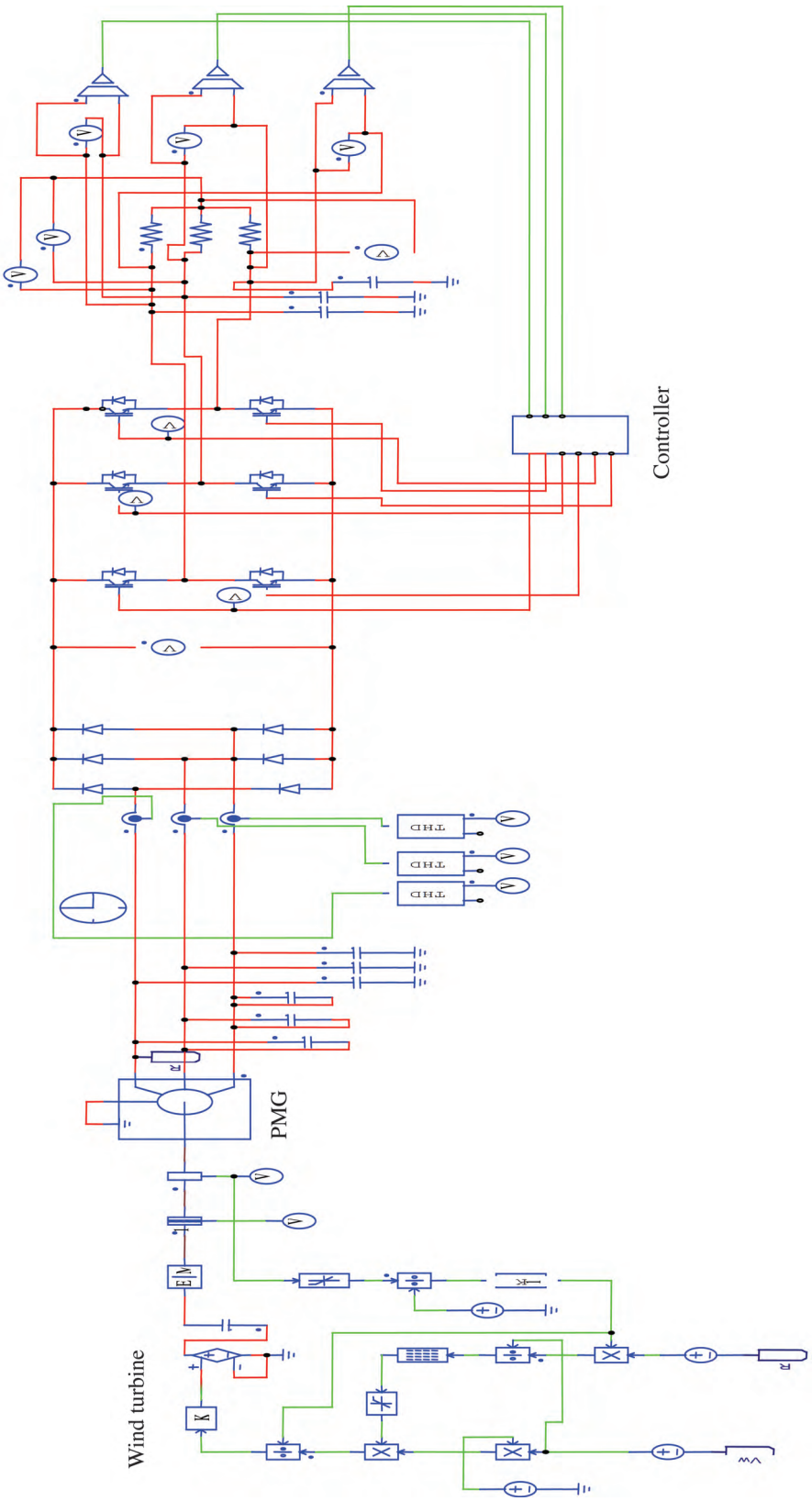

Figure 6. PSIM simulation model of conventional WECS.

Figure 7 shows the overall PSIM simulation model of the proposed WECS. This model consists of a wind turbine, a PMG, and a matrix converter with a SPWM controller. The model was simulated and analyzed for various values of wind velocity and different loading conditions.

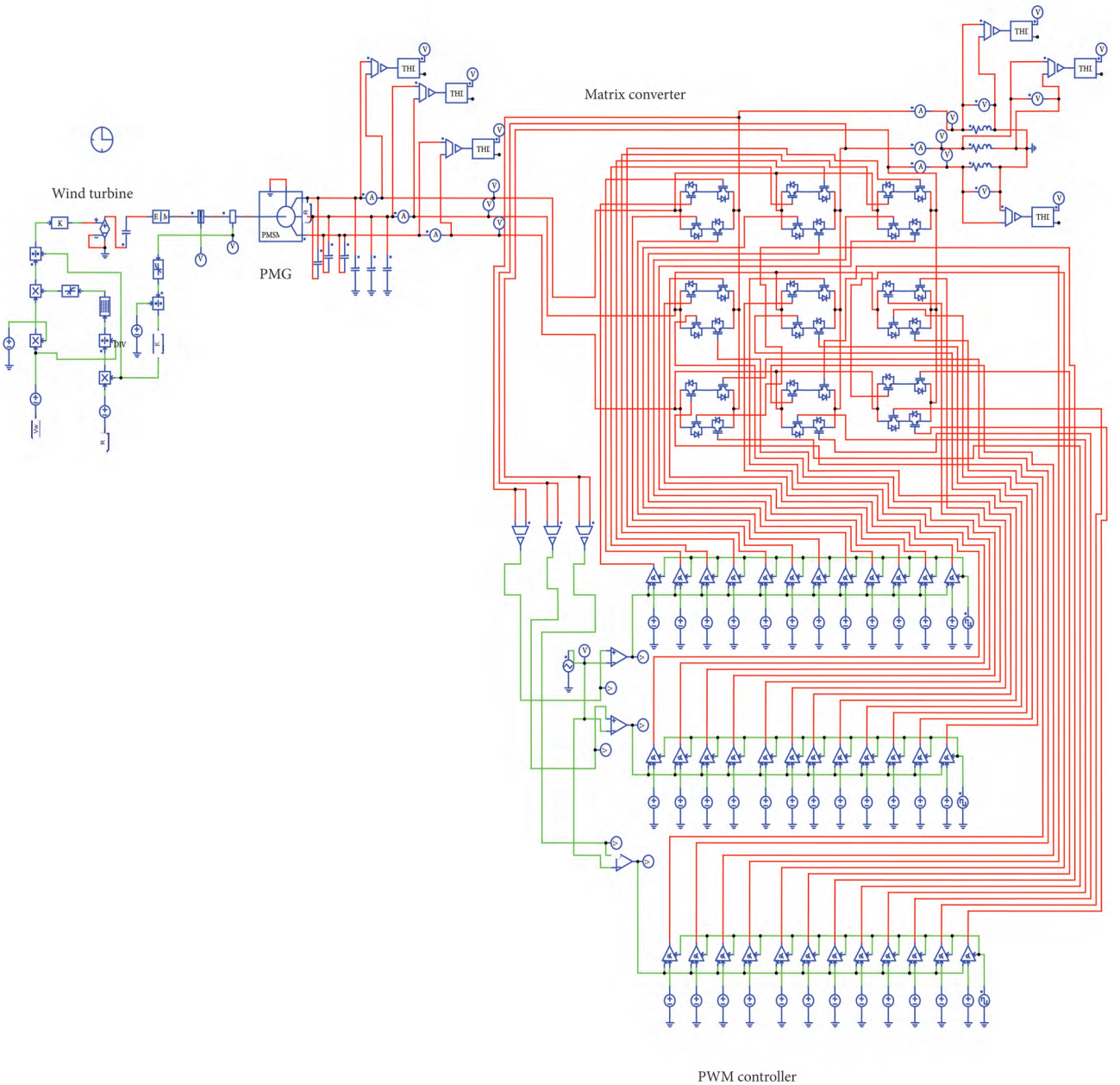

Figure 7. PSIM simulation model of proposed WECS.

Figure 8 shows the wind turbine speed in rpm for different wind velocities. The turbine speed is 42 rpm at 6 m/s and reaches the maximum speed of 123 rpm at 15 m/s. Figure 9 shows the PMG-generated voltage for different wind velocities. The generated voltage is at a maximum at 541 V at 15 m/s and at a minimum at 370 V at 7 m/s. The frequency of the generated voltage is 22 Hz at 7 m/s with a rated value of 50 Hz at

11 m/s. When the matrix converter is fed without a closed-loop controller, the frequency and amplitude of the matrix converter output varies. This is shown in Figure 10.

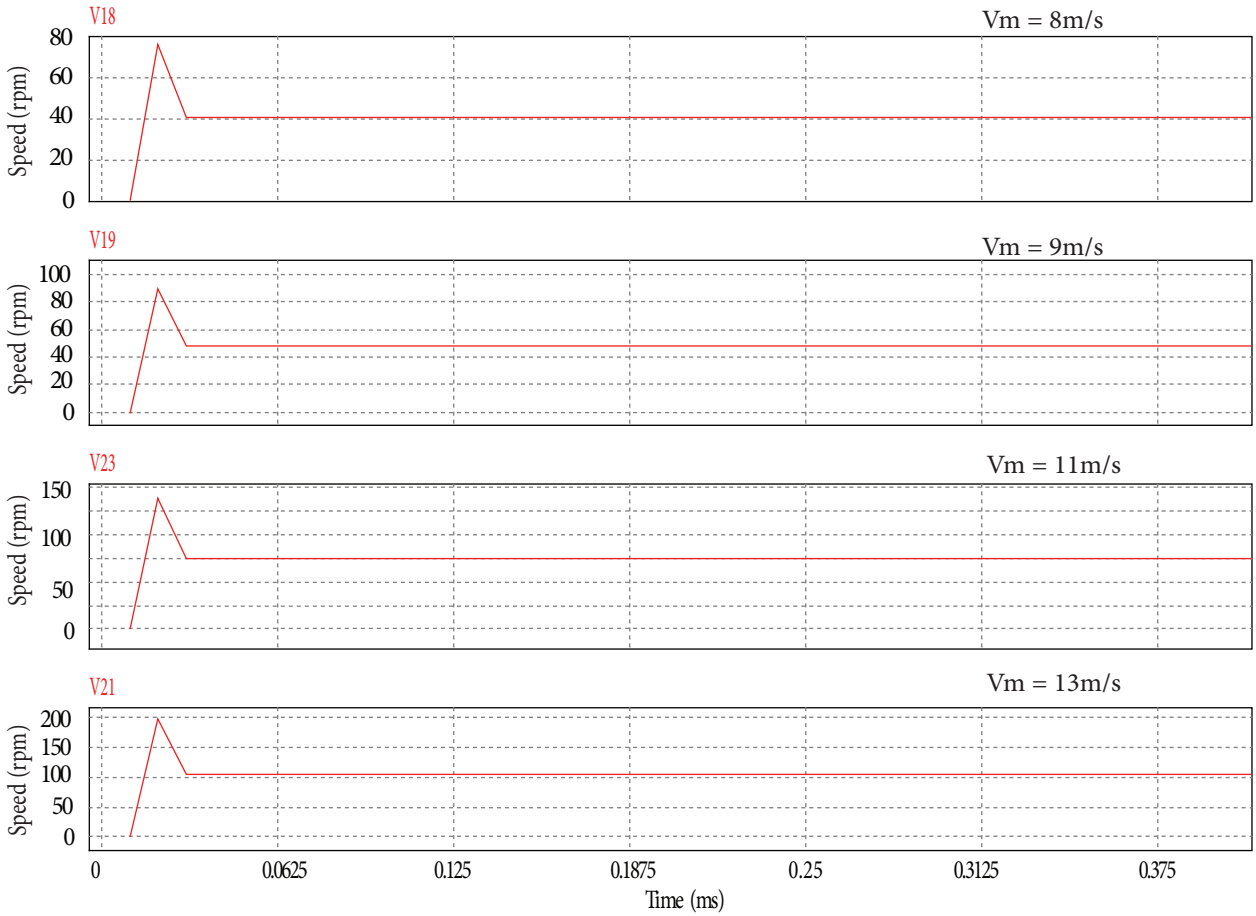

Figure 8. Wind turbine speed for different wind velocities.

To obtain the desired voltage and frequency, the matrix converter is controlled by the SPWM controller along with voltage feedback. Figure 11 shows the magnitude of the matrix converter voltage with the controller. For all values of voltage and frequency shown in Tables 1 and 2, the output voltage is converted to a fixed value of 400 V and 50 Hz. The output voltage is almost sinusoidal; hence, it has a lower value of THD and requires less filtering equipment.

Figure 12 shows the variation of PMG-generated voltage in correspondence to speed and wind velocity. At 7 m/s, the speed of the wind turbine generator is 30 rpm and the generated voltage is 370 V. At 13 m/s, the voltage is 498 V. The variation of generated voltage for different wind velocities is given in Table 1. The generated voltage frequency is at its minimum of 22 Hz at 7 m/s and its maximum of 88 Hz at 15 m/s, as shown in Table 2 and Figure 13.

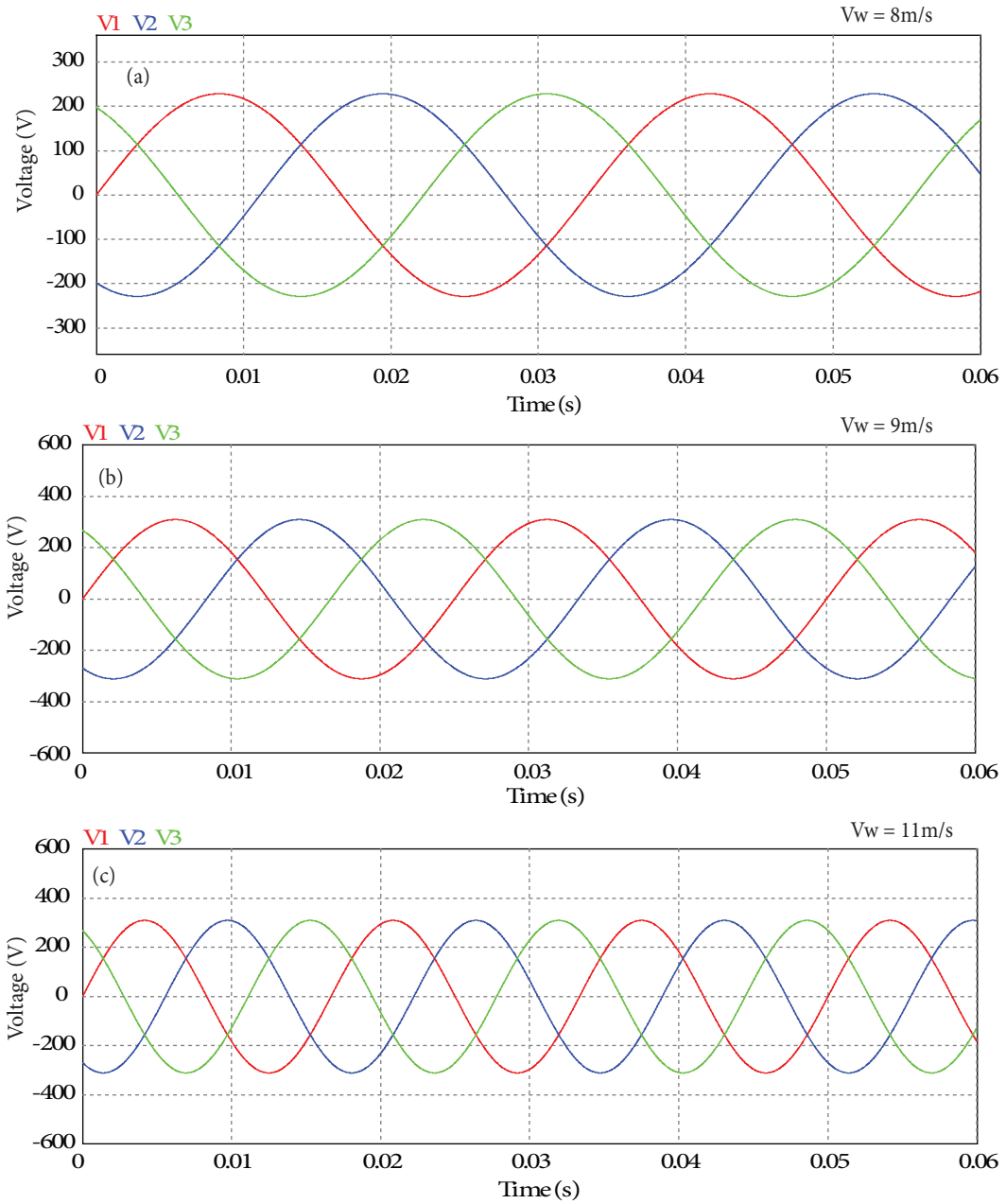

Figure 9. Simulation of PMG output voltage for wind velocities of a) 8 m/s, b) 9 m/s, and c) 11 m/s.

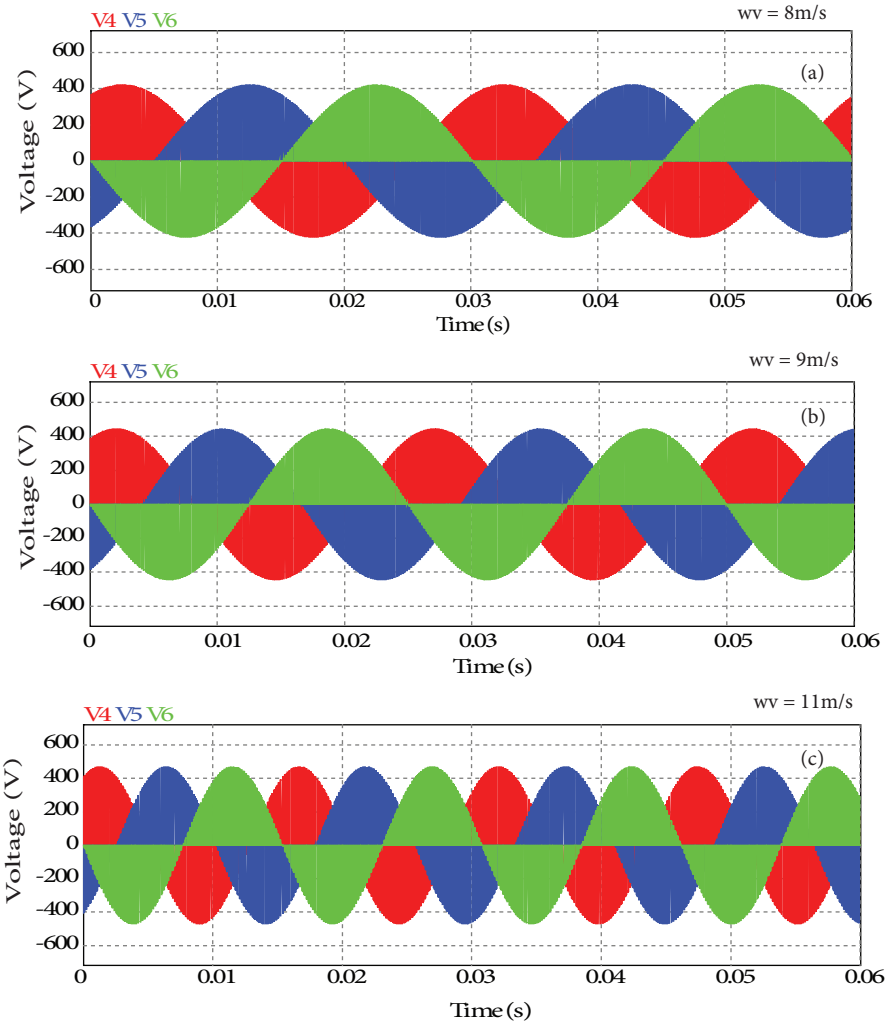

Figure 10. Simulation of matrix converter output voltage for different wind velocities.

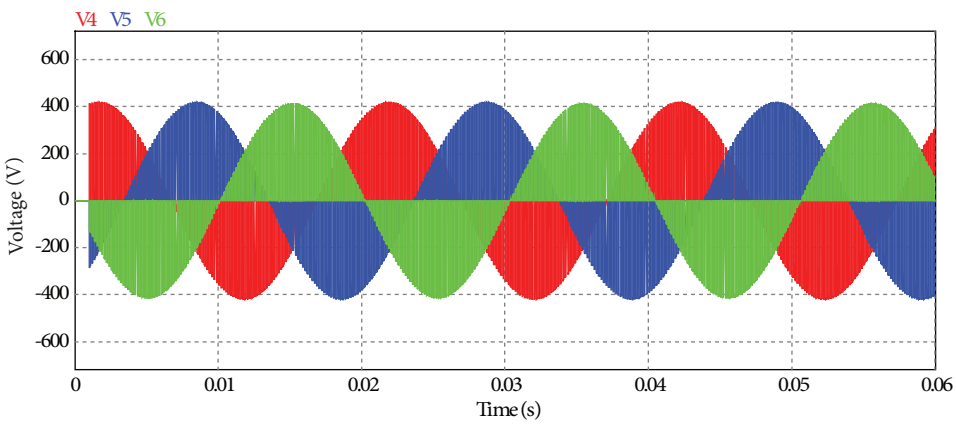

Figure 11. Matrix converter output voltage with closed-loop controller.

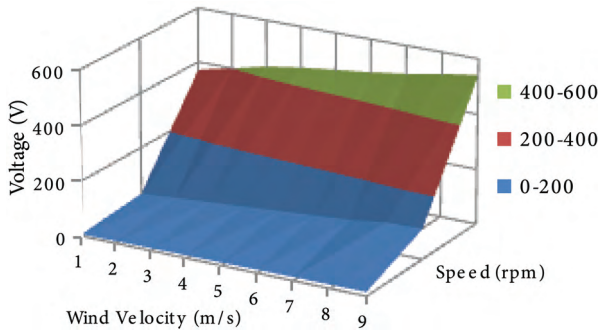

Figure 12. Variation of wind speed and generated voltage as a function of wind velocity.

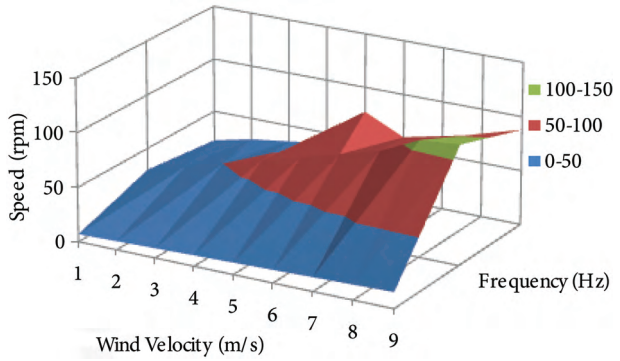

Figure 13. Speed and frequency of generated voltage as a function of wind velocity.

Table 1. Variation of speed and generated voltage as a function of wind velocity.

Wind velocity (m/s)	Speed (rpm)	Voltage (V)
7	30	370
8	42	400
9	54	430
10	60	450
11	70	465
12	82	480
13	93	498
14	107	522
15	123	541

Table 2. Speed and frequency of generated voltage as a function of wind velocity.

Wind velocity (m/s)	Speed (rpm)	Frequency (Hz)
7	30	22
8	42	30
9	54	35
10	60	40
11	70	50
12	82	60
13	93	68
14	107	76
15	123	88

The dynamic performance of the wind turbine PMG with a matrix converter was analyzed for sudden variations of wind velocity, as shown in Figure 14. This dynamic performance was examined for wind velocities of 7 m/s, 12 m/s, 9 m/s, and 8 m/s without a closed-loop controller. From these simulation results, it is clear that the matrix converter has a faster dynamic response with the varying of wind speed.

The simulation aimed to verify the performance of the proposed WECS for different loading conditions. The results of load current for R and RL loads, respectively, can be seen in Figures 15a and 15b.

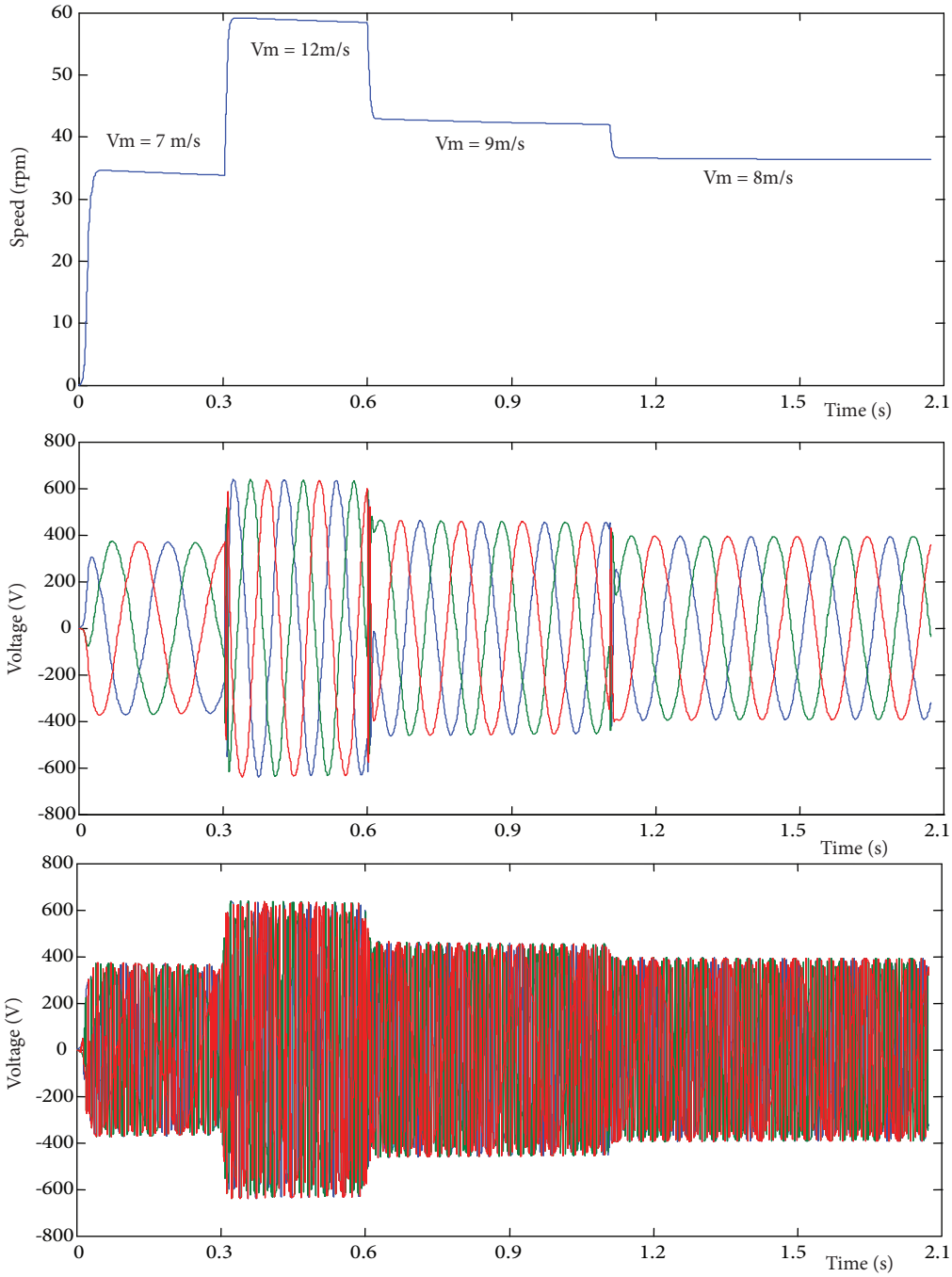

Figure 14. Dynamic responses of proposed WECS for changes in wind speed.

Figure 16 shows the variation of the input current THD of a traditional WECS and the proposed WECS. The percentage THD of the conventional system was almost 10% greater than that of the proposed WECS. This leads to a lower input power factor; hence, conduction loss in the switches is increased. As seen in Figure 17, the output voltage THD of the conventional WECS was almost 20% greater than that of the proposed WECS; this also leads to a reduction in the power quality on the output side. Hence, efficiency is reduced by 2.6%, as shown in Figure 18.

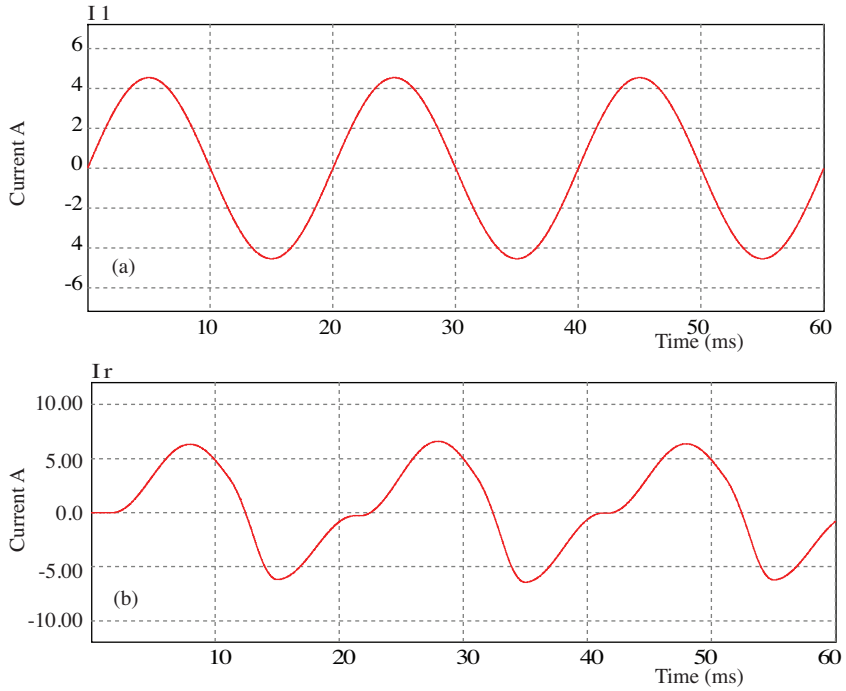

Figure 15. Simulation load current for a) R load and b) RL load.

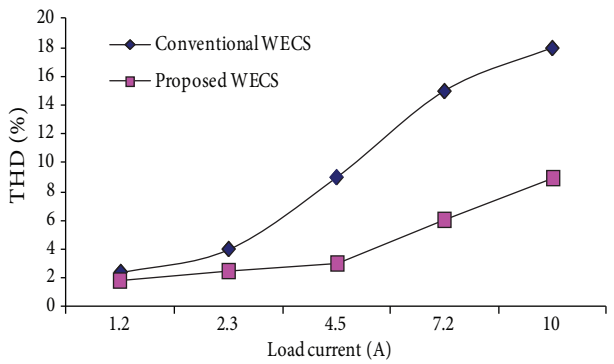

Figure 16. Input current THD (%) of matrix converter as a function of load current.

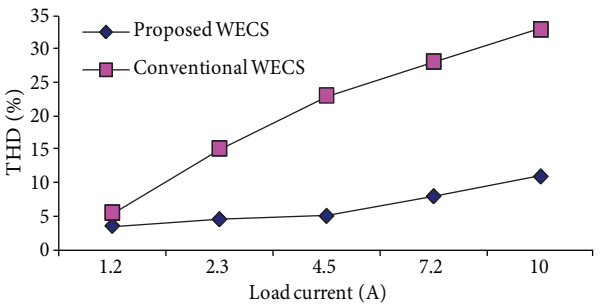

Figure 17. Output voltage THD (%) of matrix converter as a function of load current.

4. Experimental results

Figures 19a and 19b show the per phase generated voltage of the laboratory experiment setup. The PMG generates 185 V with a frequency 40 Hz at the speed of 60 rpm. This voltage is fed into the matrix converter. The matrix converter produces 140 V per phase with a frequency of 50 Hz, as shown in Figures 19c and 19d. The TMS320F2407 Digital Signal Processor is used to generate the SPWM pulses for the IGBTs in the matrix converter. The pulses generated for switches SAa and SBa are given in Figure 19b.

The experimental waveforms for the proposed WECS with an RL load are shown in Figure 20. In Figure 20a, the terminal voltage is decreased by 5 V for the load current of 1.3 A. Figures 20b and 20c show the load current of phase A and phase B.

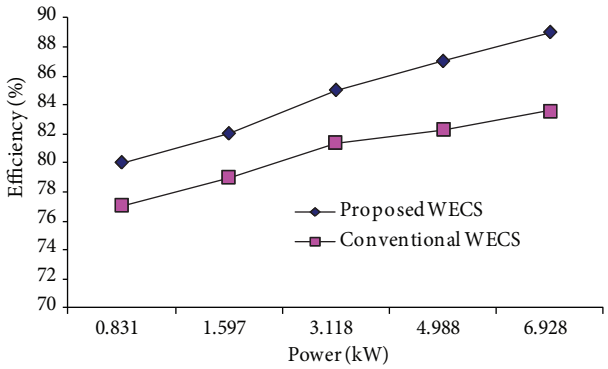

Figure 18. Simulation results of efficiency comparison.

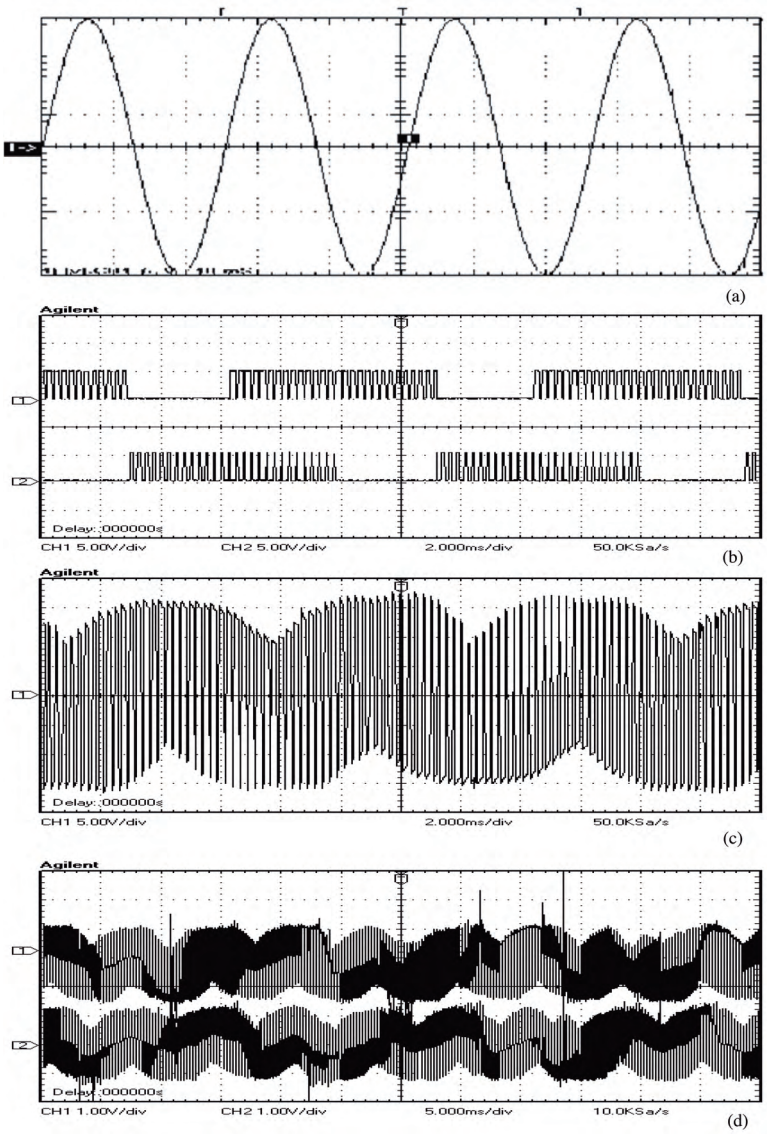

Figure 19. Experimental waveforms of 5 V/division: a) PMG-generated voltage (10 ms/division), b) gate-drive signals to IGBTs (channel 1 for switch SAa and channel 2 for switch SBa), c) per phase output voltage of matrix converter (2 ms/division), and d) line-to-line voltage of matrix converter output (1 V/division, 5 ms/division).

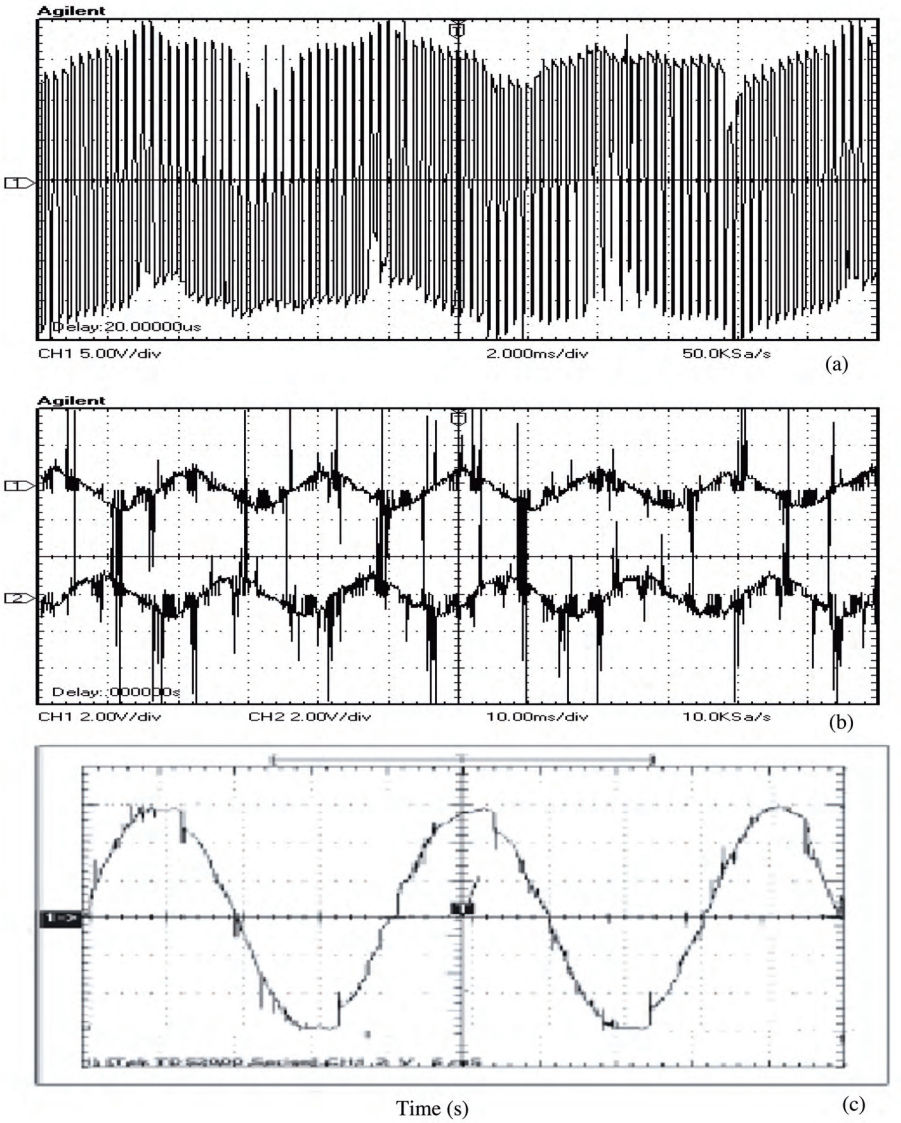

Figure 20. Experimental waveforms of proposed WECS for RL load: a) terminal voltage of matrix converter (5 V/division, 2 ms/division), b) load currents (channel 1: phase A, current 2 A/division, 10 ms/division; channel 2: phase B, current 2 A/division, 10 ms/division), and c) per phase load current for resistive load (1 A/division, 5 ms/division).

5. Conclusion

The wind turbine-driven PMG with a matrix converter was modeled using PSIM and analyzed for various values of wind velocity and different loading conditions. As the wind velocity varied, the magnitude of the generated voltage and frequency of the PMG also varied. The generated voltage was greater than 400 V for all wind velocities because of the large number of rotor poles in the PMG. The desired voltage and frequency were achieved by controlling the SPWM pulses to the matrix converter. This paper also provided a comparison of the proposed WECS with a conventional 2-stage WECS based on input and output THD levels and efficiency. When compared with the conventional WECS, the THD level of the matrix converter, both in the input and

output sides, was very low. Hence, very good power quality was achieved. Due to the improved power quality in the matrix converter, the efficiency of the proposed system is greater than that of the conventional one. The simulation results concur well with the results of the experimental setup.

Appendix

The PMG

Per phase stator resistance = 3.5 Ω
Direct axis inductance = 14.6 mH
Quadrature axis inductance = 21.2 mH

Matrix converter

Input line voltage = 480 V
Rated current = 20 A
Output frequency = 0-50 Hz
Output voltage = 400 V (line to line)

Nomenclature

ρ	Air density
A	Area swept by the blades
δ	Power angle
I_d, I_q	Stator d-q axis current
V_w	Wind velocity
λ	Tip speed ratio
ω_t	Turbine speed in rps
β	Pitch angle
C_p	Power coefficient
V_{abc}	Per phase voltages
R_{abc}	Per phase resistances
P	Differential operator (d/dt)
λ_{abc}	Flux linkages in the phases
V_{jn}	Per phase load voltage
ω_r	Rotor speed in rps
R_s	Per phase stator resistance
L_s	Per phase stator inductance
ψ_m	Magnetizing flux linkage

References

[1] N. Yamamura, M. Ishida, T. Hori, "A simple wind power generating system with permanent magnet type synchronous generator", Proceedings of IEEE International Conference on Power Electronics and Drive Systems, Vol. 2, pp. 849-854, 1999.

[2] K. Tan, S. Islam, "Optimum control strategies in energy conversion of PMSG wind turbine system without mechanical sensors", IEEE Transactions on Energy Conversion, Vol. 19, pp. 392-399, 2004.

[3] B.S. Borowy, Z.M. Salameh, "Dynamic response of a stand-alone wind energy conversion system with battery energy storage to a wind gust", IEEE Transactions on Energy Conversion, Vol. 12, pp. 73-78, 1997.

[4] A.B. Raju, K. Chatterjee, B.G. Fernandes, "A simple maximum power point tracker for grid connected variable speed wind energy conversion system with reduced switch count power converter", IEEE Power Electronics Specialist Conference, Vol. 2, pp. 748-753, 2003.

[5] M. Chinchilla, S. Arnaltes, J.C. Burgos, "Control of permanent-magnet generators applied to variable-speed wind-energy systems connected to the grid", IEEE Transactions on Energy Conversion, Vol. 21, pp. 130-135, 2006.

[6] S.M. Barakati, M. Kazerani, J.D. Aplevich, "Maximum power tracking control for a wind turbine system including a matrix converter", IEEE Transactions on Energy Conversion, Vol. 24, pp. 705-713, 2009.

[7] N. Yamamura, M. Ishida, T. Hori, "A simple wind power generating system with permanent magnet type synchronous generator", IEEE International Conference on Power Electronics and Drive Systems, Vol. 2, pp. 849-854, 1999.

[8] H. Polinder, F.F.A. Vander Pijl, G.J. DeVilder, P. Tavner, "Comparison of direct-drive and geared generator concepts for wind turbines", IEEE Transactions on Energy Conversion, Vol. 21, pp. 725-733, 2006.

[9] L. Helle, K.B. Larsen, A.H. Jorgensen, S. Munk-Nielsen, F. Blaabjerg, "Evaluation of modulation schemes for three-phase to three-phase matrix converters", IEEE Transactions on Industrial Electronics, Vol. 51, pp. 158-171, 2004.

[10] S.M. Barakati, J.D. Aplevich, M. Kazerani, "Controller design for a wind turbine system including a matrix converter", IEEE Power Engineering Society General Meeting, pp. 1-8, 2007.

[11] M.E.I. Mokadem, V. Courtecuisse, C. Saudemont, B. Robyns, J. Deuse, "Experimental study of variable speed wind generator contribution to primary frequency control", Renewable Energy, Vol. 34, pp. 833-844, 2009.

[12] A. Jahangiri, A. Radan, M. Haghshenas, "Synchronous control of indirect matrix converter for three-phase power conditioner", Electric Power Systems Research, Vol. 80, pp. 857-868, 2010.

[13] R. Bharanikumar, R. Senthil Kumar, A.N. Kumar, "Impedance source inverter for wind turbine driven permanent magnet generator", Power System Technology and IEEE Power India Conference, pp. 1-7, 2008.

[14] R. Krishnan, Electric Motor Drives: Modeling, Analysis, and Control, New Jersey, Prentice Hall, 2007.

[15] H. Karaca, R. Akkaya, "Control of Venturini method based matrix converter in input voltage variations", Proceedings of International MultiConference of Engineers and Computer Scientists, Vol. 2, 2009.

[16] M. Jussila, H. Tuusa, "Comparison of simple control strategies of space-vector modulated indirect matrix converter under distorted supply voltage", IEEE Transactions on Power Electronics, Vol. 22, pp. 139-148, 2007.

[17] Y.D. Yoon, S.K. Sul, "Carrier-based modulation technique for matrix converter", IEEE Transactions on Power Electronics, Vol. 21, pp. 1691-1703, 2006.

[18] P.W. Wheeler, J. Rodriguez, J.C. Clare, L. Empringham, A. Weinstein, "Matrix converter - a technology review", IEEE Transactions on Industrial Electronics, Vol. 49, pp. 276-288, 2002.

[19] R. Vargas, U. Ammann, J. Rodríguez, "Predictive approach to increase efficiency and reduced switching losses on matrix converters", IEEE Transactions on Power Electronics, Vol. 24, pp. 894-892, 2009.